*J. Chem. Sci.* (2020)132:125
https://doi.org/10.1007/s12039-020-01830-0


REGULAR ARTICLE

# Macrocyclic butterfly iron cluster complexes: electrochemical investigations

TASHIKA AGARWAL and SANDEEP KAUR-GHUMAAN*
Department of Chemistry, University of Delhi, Delhi 110 007, India
E-mail: skaur@chemistry.du.ac.in

MS received 19 April 2020; revised 4 July 2020; accepted 15 July 2020

**Abstract.** The article primarily highlights the electrocatalytic activity towards proton reduction of macrocyclic tetranuclear iron complexes $[Fe_2(\mu\text{-}S(CH_2)_nS\text{-}\mu)(CO)_6]_2$ (n = 4, **1** and n = 6, **2**) with both acetic acid and trifluoroacetic acid as proton sources. Further, the electrochemical results have been compared with the analogous pentanedithiolate-bridged tetranuclear complex, $[Fe_2(\mu\text{-}S(CH_2)_5S\text{-}\mu)(CO)_6]_2$ **A**. The turnover frequency (*TOF*, acetic acid) for complexes **1** and **2** was found to be 5.7 $h^{-1}$ and 9.1 $h^{-1}$, respectively. An ECEC catalytic cycle (acetic acid) has been proposed for the tetranuclear iron complexes based on the experimental data and known literature.

**Keywords.** Macrocycles; iron cluster compounds; electrocatalysis; hydrogen; homogeneous catalysis.

## 1. Introduction

Platinum catalysts are used to produce hydrogen *via* water electrolysis.[1] Though this is considered to be one of the cleanest ways of producing hydrogen, it is limited by the cost and availability of platinum. Therefore, with an aim to develop cheap, efficient and robust catalysts, a large number of structural and functional biomimetic models of Fe-only hydrogenases have been developed over the last three decades.[2] These organometallic bio-inspired mimics are mostly dinuclear[3] but examples of mononuclear[4] and trinuclear[5] iron complexes which function as active electrocatalysts for proton reduction, are also known. There are also reports of double-butterfly $Fe_2S_2$ carbonyl complexes with aliphatic chains[6–10] (consisting of alkanes or carbon chains with O, N, S, -OH groups, and organotin groups) or aromatic groups[11–13] as linkers. Examples of tetranuclear complexes with two $Fe_2S_2$ units linked *via* single sulphur atom[14] of each unit or by bidentate or cyclic phosphines,[15] are also present in literature (Figure 1). Till date, most of the double-butterfly $Fe_2S_2$ carbonyl complexes have been reported as structural mimics of the enzyme active site. The various functional tetranuclear (macrocyclic/non-macrocyclic) complexes are shown in Figure S1 (Supplementary Information).[16–22]

The tetrairon complex $(\mu,\mu\text{-ttn})[Fe_2(CO)_6]_2$ (ttn = tetrathionaphthalene) with an aromatic thiolate reported in 1977 was one of the first examples containing two $Fe_2S_2$ units.[23] Tetranuclear cyclic complexes with aliphatic thiolate linkers were first reported by Song and co-workers in 2002.[24] Electrochemical hydrogen evolution from acetic acid catalyzed by macrocyclic complexes $[Fe_2(\mu\text{-}1,5\text{-pentanedithiolate})(CO)_6]_2$ **A** and $[Fe_2(\mu\text{-}S(CH_2)_2N(^nPr)(CH_2)_2\text{-}S)(CO)_{6-x}L_x]_2$ (x = 0, **B**; L = $PPh_3$, x = 1, **C**; L = $P^nBu_3$, x = 1, **D**) was reported by Chiang and co-workers (Figure S1, Supplementary Information).[16] Non-macrocyclic catalytically active tetrairon systems include $(\mu,\mu\text{-benzene-}1,2,4,5\text{-tetrathiolato})[Fe_2(CO)_6]_2$ **E**, $(\mu,\mu\text{-benzene-}1,2,3,4\text{-tetrathiolato})[Fe_2(CO)_6]_2$ **F**, $(\mu,\mu\text{-benzene-}1,2,4,5\text{-tetrathiolato})[Fe_2(CO)_6][Fe_2(\text{-}CO)_5PPyr_3]$ **G** and $(\mu,\mu\text{-benzene-}1,2,4,5\text{-tetrathiolato})[Fe_2(CO)_5PPyr_3]_2$ **H** (where Pyr = N-pyrrolyl) (Figure S1, Supplementary Information).[17] The reduction potentials of the tetranuclear complexes **E** and **F** were found to be less negative when compared to diiron complexes, $[Fe_2(\mu\text{-pdt})(CO)_6]$ (irreversible one-electron reductions at −1.74 and −2.35 V *vs.* $Fc/Fc^+$ in

*For correspondence

*Electronic supplementary material: The online version of this article (https://doi.org/10.1007/s12039-020-01830-0) contains supplementary material, which is available to authorized users.*

Published online: 11 September 2020

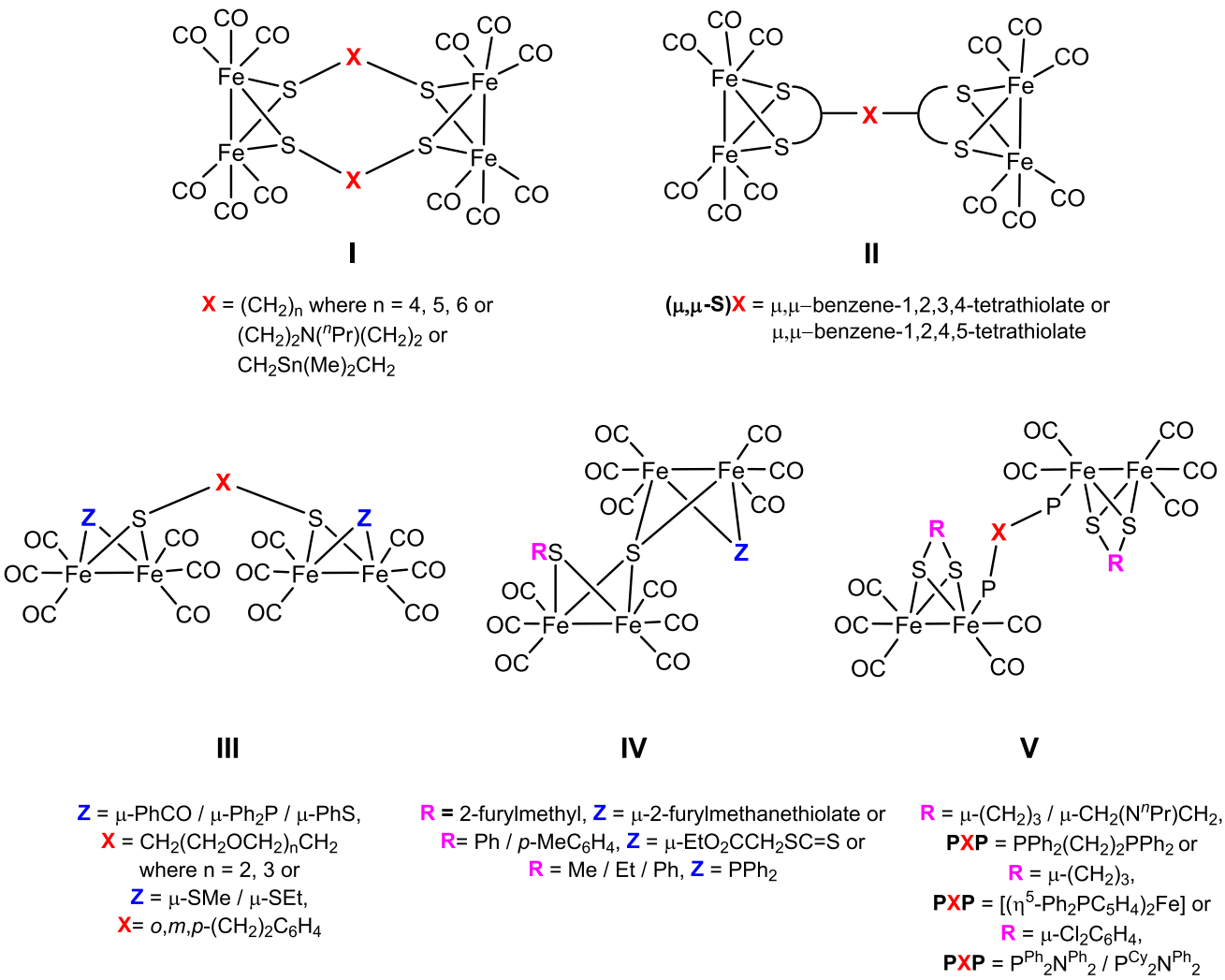


**Figure 1.** Different types of reported tetranuclear iron-thiolate complexes.

$CH_2Cl_2$)[25] and [$Fe_2$(μ-bdt)$(CO)_6$] (reversible two-electron reduction at −1.44 *vs.* $Fc/Fc^+$ in $CH_2Cl_2$)[26] (pdt: propanedithiolate and bdt: benzenedithiolate). The bulkiness of the dithiolato linker connecting the two $Fe_2S_2$ sites is also known to play a pivotal role in stabilization of the rotated/semi-rotated states of such complexes.[6a] Hence, electrochemical properties of two known macrocyclic complexes [$Fe_2$(μ-1,4-butanedithiolate)$(CO)_6]_2$ **1**, and [$Fe_2$(μ-1,6-hexanedithiolate)$(CO)_6]_2$ **2** have been hereby studied. The electrocatalytic results of complexes **1** and **2** have been compared with the reported analogous complex [$Fe_2$(μ-1,5-pentanedithiolate)$(CO)_6]_2$ **A**.[16] Furthermore, the influence on the electrochemical and electrocatalytic properties by the systematic increase of n from 4 to 6 in complexes **A**, **1** and **2** was explored.

## 2. Experimental

### 2.1 *Materials and physical measurements*

Solvents were of reagent grade and used without further purification unless otherwise noted. $Fe_3(CO)_{12}$; 1,4-butanedithiol; 1,6-hexanedithiol; acetic acid and trifluoroacetic acid were purchased from Sigma-Aldrich and used as received. Flash chromatography was performed on Merck silica gel SI-60 Å (35–70). FTIR absorption spectra were recorded in $CH_2Cl_2$ or $CH_3CN$ between 1000 and 5000 $cm^{-1}$ at a resolution of 1 $cm^{-1}$ on a Bruker FTIR spectrometer. The $^1H$ NMR spectra were recorded with Jeol JNM-EXCP 400 spectrometer in $CDCl_3$ solvent at room temperature. The CHNS analysis was performed on Vario Micro Cube elemental analyzer (Elementar Analysensysteme GmbH, Germany).

### 2.2 *Electrochemistry*

Cyclic voltammetry (CV) was carried out using an Autolab potentiostat with a GPES electrochemical interface (Eco Chemie). The three-electrode set up consisted of a glassy carbon disc (diameter 3 mm, freshly polished) as working electrode, Pt wire as counter electrode and non-aqueous $Ag/Ag^+$ electrode (CH Instruments, 0.010 M $AgNO_3$ in acetonitrile) as the reference electrode. All solutions were prepared from dry dichloromethane (Sigma-Aldrich, spectroscopic grade, that was dried with standard methods) with 0.1 M tetrabutylammonium perchlorate (electrochemical grade) as supporting electrolyte that was dried in vacuum at 383 K. The reported potential values are referenced to the potential of the ferrocene/ferrocenium ($Fc/Fc^+$) couple. Controlled Potential Coulometry (CPC) was performed with the same instrument and three-electrode set-up described earlier. The experiment was carried out with continuous stirring and purging of argon gas at a fixed potential.

### 2.3 *Synthesis*

The complex $[Fe_2(\mu\text{-}1,4\text{-butanedithiolate})(CO)_6]_2$ **1** was synthesized according to the methods reported in literature.[9] The complex $[Fe_2(\mu\text{-}1,6\text{-hexanedithiolate})(CO)_6]_2$ **2**, although reported in literature, was synthesized *via* different experimental procedure as discussed below (Scheme 1).[6a]

In a 100 mL triple-necked round-bottom flask containing anhydrous tetrahydrofuran (25 mL) under argon atmosphere, $Fe_3(CO)_{12}$ (250 mg, 0.5 mmol) was added followed by addition of 1,6-hexanedithiol (0.075 mL, 0.5 mmol). The solution was refluxed for 1.5 h at 70 °C. Color change was observed from dark green to dark red. After cooling to room temperature, majority of the solvent was removed by rotary evaporation. The remaining solution was purified through a silica gel column using 3:7 v/v $CH_2Cl_2$ - Hexane mixture. The formation of the complexes was evident from FTIR and other spectroscopic data obtained which was similar to that reported in the literature (Figure S2, Table S1, Supplementary Information).[6a,9]

2.3a *Complex* **1**: *$[Fe_2(\mu\text{-}1,4\text{-butanedithiolate})(CO)_6]_2$*: Yield: 8% (32 mg, 0.04 mmol). Anal. Calcd for $C_{20}H_{16}Fe_4O_{12}S_4$: C, 30.03; H, 2.02. Found: C, 30.98; H, 2.14. FT-IR ($CH_2Cl_2$, $cm^{-1}$): $\nu_{CO}$ 2070 (s), 2035 (s), 1990 (s). $^1H$ NMR (400 MHz, 298 K, ppm in $CDCl_3$): 2.51–2.34 (m, 8H, -S-$CH_2$-), 1.67–1.24 (m, 8H, -$CH_2$-).

2.3b *Complex* **2**: *$[Fe_2(\mu\text{-}1,6\text{-hexanedithiolate})(CO)_6]_2$*: Yield: 11% (47 mg, 0.054 mmol). Anal. Calcd for $C_{24}H_{24}Fe_4O_{12}S_4$: C, 33.67; H, 2.83. Found: C, 33.89; H, 3.11. FT-IR ($CH_3CN$, $cm^{-1}$): $\nu_{CO}$ 2070 (s), 2034 (s), 1990 (s). $^1H$ NMR (400 MHz, 298 K, ppm in $CDCl_3$): 2.51–2.49 (m, 8H, -S-$CH_2$-), 1.59–1.29 (m, 16H, -$CH_2$-).

## 3. Results and Discussion

### 3.1 *Synthesis and characterization*

Synthesis of complexes $[Fe_2(\mu\text{-}1,4\text{-butanedithiolate})(CO)_6]_2$ **1** and $[Fe_2(\mu\text{-}1,6\text{-hexanedithiolate})(CO)_6]_2$ **2** was carried out using Schlenk-line techniques with triirondodecacarbonyl ($Fe_3CO_{12}$) and the dithiols as reactants. The FTIR data for complexes completely support their formation with $\nu_{CO}$ frequencies similar to the values reported in the literature (Table S1, Supplementary Information).[6a,9] It was observed that the chain length of the bridging thiols did not influence the carbonyl stretching frequencies to a large extent. The $^1H$ NMR (in $CDCl_3$) data for complexes **1** and **2** displayed chemical shifts in the

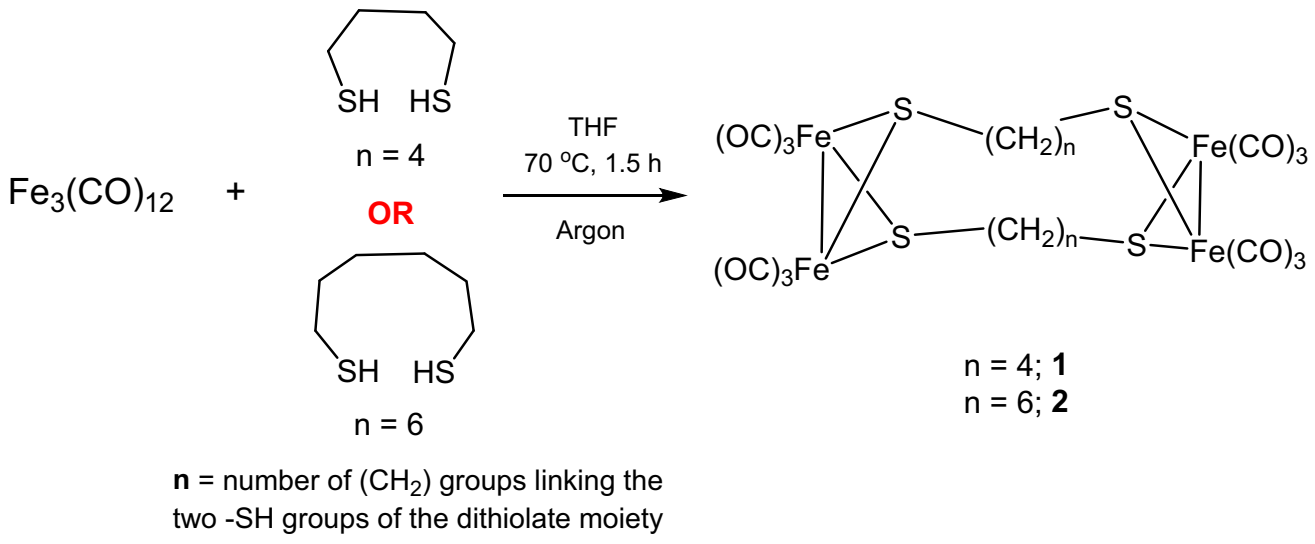


**Scheme 1.** Synthetic route for complexes **1** and **2**.

range of 1.2 to 2.6 ppm corresponding to aliphatic protons present in the bridging dithiols (Figure S2, Supplementary Information). The peaks for the methylene protons attached to μ-S atoms appear downfield (at ~2.5 ppm).[6a]

### 3.2 *Electrochemical investigations*

Very few double butterfly $Fe_2S_2$ carbonyl complexes have been studied for electrocatalytic proton reduction activity (Table 1).[16–22] The proton sources employed in the electrocatalytic studies have usually been strong acids except in the case for macrocyclic complexes **B**, **C**, and **D**; wherein acetic acid has been used.[16] The all-carbonyl non-macrocyclic complexes **E** and **F** were found to be electrocatalytically inactive in the presence of acetic acid (Table 1).[17] Herein, we examine complexes [$Fe_2$(μ-1,4-butanedithiolate)$(CO)_6]_2$ **1** and [$Fe_2$(μ-1,6-hexanedithiolate)$(CO)_6]_2$ **2** for proton reduction catalysis *via* cyclic voltammetric measurements and further study the influence of carbon chain length of the bridging thiol ligands on electrocatalysis.

The electrocatalytic studies for complexes **1** and **2** were carried out in $CH_2Cl_2$ due to poor solubility in the other solvents. Complex **1** displayed single irreversible two-electron reduction peak at −1.86 V (*vs.* $Fc/Fc^+$) and oxidation peaks at +0.63 and +1.96 V (*vs.* $Fc/Fc^+$) without acid addition. The two-electron reduction was assigned based on the bulk electrolysis experiment (Figure S3, Supplementary Information).[16] The consumption of two electrons per molecule indicates that both the $Fe_2S_2$ units are reduced in one step

**Table 1.** Electrochemical data for tetranuclear sulphur-bridged iron-carbonyl complexes in $CH_2Cl_2$ solution (*vs.* $Fc/Fc^+$).

| Complex | $E_{pc}^{red}$ (V) | Acid used | $E_{cat}$ (V) | Ref |
|---|---|---|---|---|
| [$Fe_2$(μ-1,4-butanedithiolate)$(CO)_6]_2$ **1** | − 1.86 | $CH_3COOH$ | − 1.88 | This work |
| | | $CF_3COOH$ | − 1.46 | This work |
| | | | − 1.88 | |
| [$Fe_2$(μ-1,6-hexanedithiolate)$(CO)_6]_2$ **2** | − 1.95 | $CH_3COOH$ | − 2.18 | This work |
| | | $CF_3COOH$ | − 1.61 | This work |
| | | | − 2.02 | |
| [$Fe_2$(μ-1,5-pentanedithiolate)$(CO)_6]_2$ **A** | − 1.97 | $CH_3COOH$ | − 1.90 | [16] |
| [$Fe_2$(μ-$S(CH_2)_2N^nPr(CH_2)_2S)(CO)_6]_2$ **B** | − 1.90 | $CH_3COOH$ | − 1.84 | [16] |
| [$Fe_2$(μ-$S(CH_2)_2N^nPr(CH_2)_2S)(CO)_5PPh_3]_2$ **C** | − 2.17 | $CH_3COOH$ | − 2.11 | [16] |
| [$Fe_2$(μ-$S(CH_2)_2N^nPr(CH_2)_2S)(CO)_5P^nBu_3]_2$ **D** | − 2.32 | $CH_3COOH$ | − 2.25 | [16] |
| (μ,μ-benzene-1,2,4,5-tetrathiolato)[$Fe_2(CO)_6]_2$ **E** | − 1.38 [a] | $CH_2ClCOOH$ | − 1.81 | [17] |
| | − 1.66 [a] | | | |
| | | $CHCl_2COOH$ | − 1.50 [b] | [17] |
| | | | − 1.75 [b] | |
| | | $CCl_3COOH$ | − 1.50 [b] | [17] |
| | | | − 1.75 [b] | |
| | | $CF_3COOH$ | − 1.38 | [17] |
| (μ,μ-benzene-1,2,3,4-tetrathiolato)[$Fe_2(CO)_6]_2$ **F** | − 1.40 [a] | $CF_3COOH$ | − 1.50 [b] | [17] |
| | − 1.66 [a] | | | |
| (μ,μ-benzene-1,2,4,5-tetrathiolato)[$Fe_2(CO)_6$][$Fe_2(CO)_5PPyr_3$] **G** | − 1.42 [a] | $CF_3COOH$ | − 1.60 [b] | [17] |
| | − 1.70 [a] | | | |
| (μ,μ- benzene-1,2,4,5-tetrathiolato)[$Fe_2(CO)_5PPyr_3]_2$ **H** | − 1.47 [a] | $CF_3COOH$ | − 1.60 [b] | [17] |
| | − 1.79 [a] | | | |
| [$Fe_2(CO)_6$(μ-$SCH_2)_2NCH_2CH_2N$(μ-$SCH_2)_2$]$Fe_2(CO)_6$ **I** [c,d] | − 1.42 | $CF_3SO_3H$ | − 1.18 | [18] |
| | − 1.51 | | − 1.70 [b] | |
| [{$Fe_2(CO)_5$(μ-$SCH_2)_2NCH_2CH_2N$(μ-$SCH_2)_2Fe_2(CO)_5$}($Ph_2PCH_2)_2$] **J** | − 2.08 | $CF_3SO_3H$ | − 1.28 | [19] |
| | | | − 2.00 | |
| [$Fe_2(CO)_5$(μ-($SCH_2)_2CH_2$)($Ph_2PCH_2$)]$_2$ **K** [d] | − 1.94 | $CF_3SO_3H$ | − 1.94 | [20] |
| [$Fe_2(CO)_5$(μ-($SCH_2)_2N^nPr$)($Ph_2PCH_2$)]$_2$ **L** [d] | − 1.93 | $CF_3SO_3H$ | − 1.25 | [20] |
| | | | − 2.00 | |
| [$\mu_4$-Sulfido-bis{(μ-2-furylmethanethiolato)bis[tricarbonyliron] (Fe-Fe)}] **M** [c] | − 1.80 | $CH_3COOH$ | − 2.33 | [21] |
| | − 2.53 | | | |
| | | $CF_3COOH$ | − 1.47 | [21] |

[a] $E_{1/2}$ values; [b] approximate values taken from CV curves; [c] CVs performed in $CH_3CN$; [d] *vs.* Ag/0.001M $AgNO_3$.

($Fe^{I}Fe^{I} \rightarrow Fe^{I}Fe^{0}$) at ~ −1.86 V and further the two $Fe_2S_2$ units are identical and mutually independent as they are associated through alkyl linkers. Similarly, for complex **2**, reduction peak appeared at −1.95 V (*vs.* $Fc/Fc^{+}$) while the oxidation peaks appeared at +0.86 and +1.74 V (*vs.* $Fc/Fc^{+}$). The linearity of Randles-Sevick plot for the reduction peaks of complexes **1** and **2** indicated diffusion-based electrochemical systems (Figure S4, Supplementary Information).[27] Both the complexes were tested for proton reduction activity in acetic acid ($CH_3COOH$) as well as trifluoroacetic acid ($CF_3COOH$).[28]

Adding 5 mM $CH_3COOH$ to complex **1**, two reduction peaks were observed at −1.88 and −2.36 V (*vs.* $Fc/Fc^{+}$) (Figure 2). On gradual addition of higher equivalents of acid, a cathodic shift in the catalytic peaks was noticed. The rise in catalytic currents on subsequent acid addition confirmed proton reduction activity although the peak at more negative potential (−2.36 V) gradually diminished with increasing acid concentration. Complex **2** also exhibited successful electrocatalysis with $CH_3COOH$ as $H^{+}$ source wherein $E_{cat}$ was found to be −2.18 V (*vs.* $Fc/Fc^{+}$) (Figure 3). CVs for blank $CH_3COOH$ in the absence of **1** and **2** displayed poor currents in the potential range suggesting that both the complexes are active electrocatalysts (Inset, Figures 2 and 3).[29–31] On overlaying the $i_c$ / $i_p$ *vs.* acid concentration (in mM) plot for complexes **1** and **2**, it can be assumed that both the catalysts are equally efficient towards proton reduction

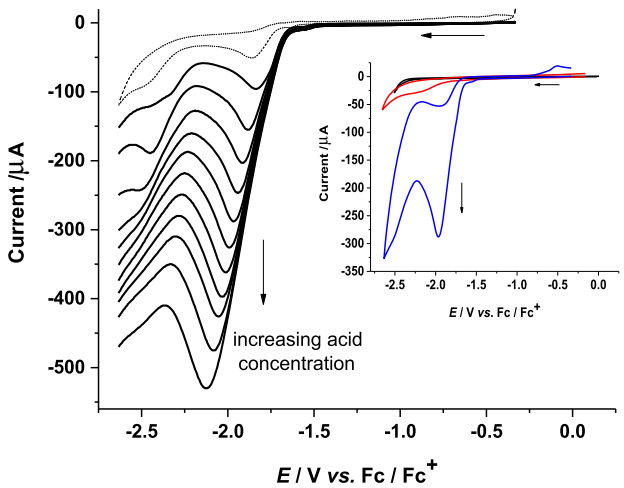


**Figure 2.** CV for complex **1** (1.13 mM) without acid (- - -) and voltammograms with increasing amounts of $CH_3COOH$ (5-52 mM) in $CH_2Cl_2$ at a scan rate of 0.1 V $s^{-1}$. Inset: CVs for $CH_2Cl_2$ (—), $CH_2Cl_2$ / 22 mM $CH_3COOH$ (—) and $CH_2Cl_2$ / 22 mM $CH_3COOH$ / 1.13 mM complex **1** (—).

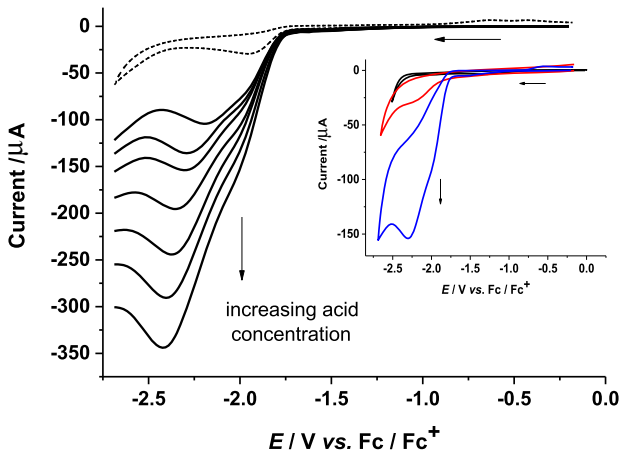


**Figure 3.** CV for complex **2** (1 mM) without acid (- - -) and voltammograms with increasing amounts of $CH_3COOH$ (6 - 60 mM) in $CH_2Cl_2$ at a scan rate of 0.1 V $s^{-1}$. Inset: CVs for $CH_2Cl_2$ (—), $CH_2Cl_2$/20 mM $CH_3COOH$ (—) and $CH_2Cl_2$/20 mM $CH_3COOH$/1 mM complex **2** (—).

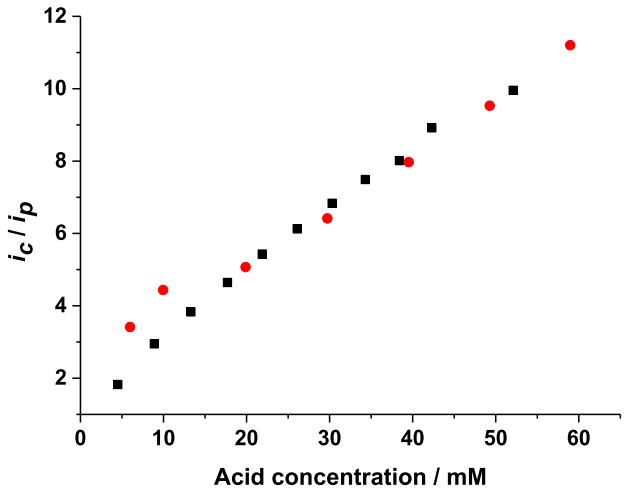


**Figure 4.** Plots of $i_c/i_p$ *vs.* [$CH_3COOH$]/mM for complexes **1** (■) (1.13 mM) and **2** (●) (1 mM) in $CH_2Cl_2$.

with $CH_3COOH$ as proton source ($i_c$ is catalytic current in presence of acid and $i_p$ is peak current value in absence of acid) (Figure 4).[32] However, the catalytic efficiency (C.E.) for **1** and **2** in $CH_3COOH$ was found to be 0.46–0.24 and 0.57–0.21, respectively.[27]

The value of observed rate constant $k_{obs}$ at the maximum acid addition value was calculated using Equation (1) where, $i_{cat}$ is catalytic current in presence of acid, $i_p$ is peak current value in absence of acid, $n$ is number of electrons required for generating one mole of $H_2$ (here, $n = 2$), $F$ is Faraday constant, ν is scan rate in $Vs^{-1}$, $R$ is ideal gas constant, $T$ is the temperature in Kelvin and $k_{obs}$ is observed rate constant in $s^{-1}$.[27, 28] In many reports, the calculated value of $k_{obs}$ is also referred to as turnover frequency (*TOF*) of the catalyst.[29, 30]

$$\frac{i_{cat}}{i_p} = \frac{n}{0.4463}\sqrt{\frac{RTk_{obs}}{Fv}} \quad (1)$$

A linear plot of $i_c$ / $i_p$ *vs.* acetic acid concentration (in mM) for complexes **1** and **2** is for a scan rate of 0.1 V $s^{-1}$ is shown in Figure 4. The turnover frequencies (at the highest acid concentration investigated) as calculated from Equation (1) were found to be 19.5 $s^{-1}$ and 24.7 $s^{-1}$ for complexes **1** and **2**, respectively.[31]

Complexes **1** and **2** were also found to be equally stable in the presence of a moderately strong acid ($CF_3COOH$), displaying catalytic peaks at − 1.46, − 1.88 and − 1.61, − 2.02 V; respectively (Figures S5 and S6, Supplementary Information). Usually, in cases wherein $CF_3COOH$ is employed as proton source in $CH_3CN$ solvent, the second catalytic peak is attributed to the homoconjugation phenomenon.[33, 34] On comparing electrocatalytic currents in presence of complexes **1** and **2** to blank $CF_3COOH$ (in $CH_2Cl_2$) it was confirmed that the complexes are functionally active towards proton reduction (Figures S7 and S8, Supplementary Information). In this case, catalytic currents were higher for complex **2** than **1** as indicated by the $i_c$ / $i_p$ *vs.* acid concentration (in mM) plot (Figure S9, Supplementary Information).

To further establish the catalytic generation of hydrogen, controlled-potential electrolysis was carried out for complexes **1** and **2** in $CH_3COOH$. Though some uncatalyzed proton reduction was detected on the addition of acid but in the presence of the catalyst, the higher value of charge for the specified time period supports the catalytic activity of the complexes (Figure 5). The values of turnover frequency (*TOF*) and turnover number (TON) for complexes **1** and **2** were

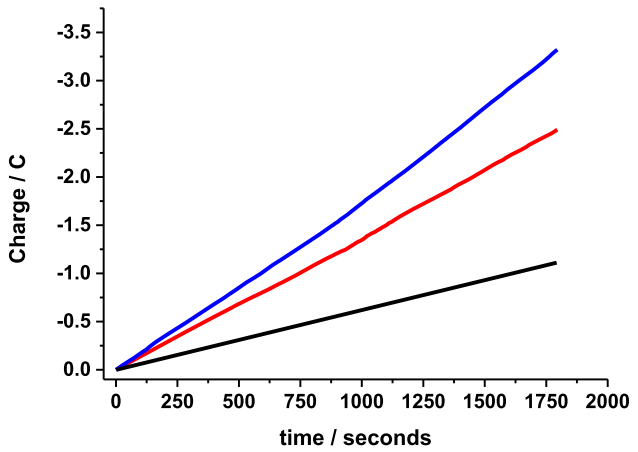


**Figure 5.** Plots of charge (Q)/C *vs.* time (t)/seconds for 1.25 mM $CH_3COOH$ (—) and 0.25 mM complex **1** (—) and **2** (—) with 1.25 mM $CH_3COOH$ in $CH_2Cl_2$ at electrolysis potential of -2 V (1.25 mM = 10 eq and solution volume = 10 mL).

calculated using Equations (2) and (3).[35–38] The values of *TOF* and TON for complex **1** were 5.72 $h^{-1}$ and 2.86 in acetic acid, respectively. For complex **2**, the respective values of *TOF* and TON were 9.07 $h^{-1}$ and 4.53. Hence, the coulometric results hint towards better turnovers for complex **2** over complex **1**.

$$\mathrm{TOF} = \frac{\Delta C}{F * n_1 * n_2 * t} \quad (2)$$

$$\mathrm{TON} = \mathrm{TOF} * t \quad (3)$$

Where, ΔC is the difference between charge from catalyst solution and charge from solution in absence of catalyst during electrolysis, $F$ is Faraday's constant, $n_1$ is the number of moles of electrons required to generate one mole of $H_2$, $n_2$ is the number of moles of catalyst in solution and $t$ is the duration of electrolysis.

For the analogous complex **B**, a linear Q-t plot was obtained in the first one hour resulting in a TON of 4.1 $mol^{-1}$ $h^{-1}$ in presence of $CH_3COOH$ (in $CH_2Cl_2$) at room temperature.[16] In the electrolysis data for non-macrocyclic tetranuclear complexes **I** and **J** (both 1 mM), after about 1.5 h, complex **I** gave ca. 60 turnovers of $H_2$ while complex **J** effectively displayed ca. 80–90 turnovers in presence of $CF_3SO_3H$ (in $CH_2Cl_2$).[18,19] During coulometry of binuclear complexes **K** and **L** (both 1 mM), the catalytic activity for **K** lasted for 50 min while for **L**, it went up till 1.5 h. This corresponded to ca. 8 turnovers for **K** and 24 for **L** in presence of $CF_3SO_3H$ (in $CH_2Cl_2$).[20]

The model complexes with tetranuclear iron centers were found to exhibit moderate catalytic activity towards $H^+$ reduction.[16–22] A clear trend in reduction potential of complexes was not observed with the increasing chain length of dithiols for complexes **A**, **1** and **2**; though it was expected that as number of carbon atoms increased in the bridging dithiolate group, the reduction should occur at more negative potentials. In our report, it was clearly established that complex **2** appeared to be more active than **1** in both weak as well as a moderately strong acid source. As it has already been proposed by Chiang and co-workers for complex **B** that the presence of azanitrogen (-NR-) site does not play any role in the catalytic process, hence the possible site for protonation could be the iron center for complexes **A**, **1** and **2**.[16] Based on literature and the electrocatalytic data, an ECEC mechanism (acetic acid) is proposed for complexes **A**, **1** and **2** (general structure = **X**) wherein reduction at one iron centre of each $Fe_2S_2$ unit results in the intermediate $\mathbf{X^{2-}}$ ($[\{Fe^0Fe^I\}^-]_2$) (first reduction step is also because the catalytic peaks with acetic acid are cathodically

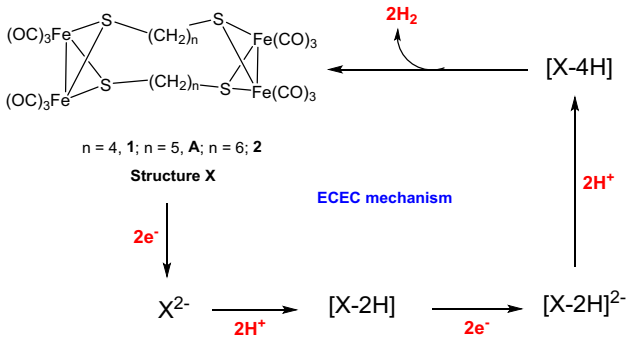


**Scheme 2.** Plausible catalytic cycle for proton reduction (acetic acid) by complexes **A**, **1** and **2**.

shifted in comparison to the neutral complex reduction peaks). This reduced species is then protonated by two $H^+$ ions and due to a rapid protonation event, a positive shift in potential is noted. Consequently, another reduction step follows, resulting in the intermediate **[X-2H]$^{2-}$** which is ultimately protonated to lead to the transient ($\eta_2$-$H_2$)FeFe species. In the final step, two molecules of hydrogen are released (Scheme 2).[16, 20]

Further, in the presence of $CF_3COOH$, the anodically shifted catalytic peaks in comparison to the neutral complex reduction peaks indicate a first protonation (chemical, C) step during the catalytic cycle.[39] Hence, a different mechanism is operative in the case of trifluoroacetic acid.

## 4. Conclusions

The steric bulk of the dithiolate group on the diiron center influences the geometry and redox properties of the $Fe_2S_2$ models, mainly by stabilization of rotated/semi-rotated states of the iron hydrogenase's active site mimics.[6a] Keeping these factors in mind, cyclic voltammetry and controlled-potential electrolysis for complexes **1** and **2** have been explored. The complexes **1** and **2** were active electrocatalysts for proton reduction with both acetic acid and trifluoroacetic acid as proton sources. The complexes displayed moderate values of *TOF* and TON with acetic acid i.e. 5.72 $h^{-1}$ and 2.86 for **1** and 9.07 $h^{-1}$ and 4.53 for **2**, respectively. The slightly better activity for complex **2** could be due to the flexibility of the system arising from the presence of larger chain length of the alkyl thiolate linker. A direct comparison of complexes **A**, **1** and **2** could not be made because no regular pattern in reduction potentials was observed. In literature, few tetranuclear models[16–22] have been studied as functional mimics for electrocatalytic proton reduction, but such systems provide tremendous scope for future studies as they can be synthetically modified to introduce other atoms in the dithiolate linker chain to provide additional proton binding sites or to tune the geometry and electronic properties of the molecule as desired. Other atoms like Sn have already been incorporated in the dithiolate linkers for tetranuclear complexes with -S-$CH_2$-Sn-$CH_2$-S- chain but such systems have not yet been exploited for proton reduction catalysis.[6c] Also, further work is necessary to establish the relation between the electronic structure of the $Fe_2S_2$ units and the catalytic mechanism for proton reduction.

## Supplementary Information (SI)

The Supplementary information includes electrochemical data and other related plots. Supplementary Information is available at www.ias.ac.in/chemsci.

## Acknowledgements

Financial support from the Council of Scientific & Industrial Research (CSIR), India (01(2957)/18/EMR-II) is gratefully acknowledged. SK-G is thankful to University of Delhi for the instrumental facilities. TA is grateful to University Grants Commission (UGC) for fellowship.

## References

1. (a) Borup R, Meyers J, Pivovar B, Kim Y S, Mukundan R, Garland N, Myers D, Wilson M, Garzon F, Wood D, Zelenay P, More K, Stroh K, Zawodzinski T, Boncella J, McGrath J E, Inaba M, Miyatake K, Hori M, Ota K, Ogumi Z, Miyata S, Nishikata A, Siroma Z, Uchimoto Y, Yasuda K, Kimijima K and Iwashita N 2007 Scientific Aspects of Polymer Electrolyte Fuel Cell Durability and Degradation *Chem. Rev.* **107** 3904; (b) Cammack R, Frey M and Robson R 2001 *Hydrogen as a Fuel: Learning from Nature* (London and New York: Taylor & Francis)
2. (a) Wittkamp F, Senger M, Stripp S T and Apfel U P 2018 [FeFe]-Hydrogenases: recent developments and future perspectives *Chem. Commun.* **54** 5934; (b) Schilter D, Camara J M, Huynh M T, Hammes-Schiffer S and Rauchfuss T B 2016 Hydrogenase Enzymes and Their Synthetic Models: The Role of Metal Hydrides *Chem. Rev.* **116** 8693; (c) Li Y and Rauchfuss T B 2016 Synthesis of Diiron(I) Dithiolato Carbonyl Complexes *Chem. Rev.* **116** 7043
3. (a) Figliola C, Male L, Horton P N, Pitak M B, Coles S J, Horswell S L and Grainger R S 2014 [FeFe]-Hydrogenase Synthetic Mimics Based on Peri-Substituted Dichalcogenides *Organometallics* **33** 4449; (b) Hsieh C H, Erdem Ö F, Harman S D, Singleton M L, Reijerse E, Lubitz W, Popescu C V, Reibenspies J H, Brothers S M, Hall M B and Darensbourg M Y 2012

Structural and Spectroscopic Features of Mixed Valent $Fe^{II}Fe^{I}$ Complexes and Factors Related to the Rotated Configuration of Diiron Hydrogenase *J. Am. Chem. Soc.* **134** 13089; (c) Wright R J, Lim C and Tilley T D 2009 Diiron Proton Reduction Catalysts Possessing Electron-Rich and Electron-Poor Naphthalene-1,8-dithiolate Ligands *Chem. Eur. J.* **15** 8518

4. (a) Natarajan M, Faujdar H, Mobin S M, Stein M and Kaur-Ghumaan S 2017 Mononuclear Iron Carbonyl Complex $[Fe(\mu\text{-bdt})(CO)_2(PTA)_2]$ with bulky phosphine ligand: A model for the [FeFe] hydrogenase enzyme active site with an inverted redox potential *Dalton Trans.* **46** 10050; (b) Weber K, Weyhermüller T, Bill E, Erdem Ö F, and Lubitz W 2015 Design and Characterization of Phosphine Iron Hydrides: Toward Hydrogen-Producing Catalysts *Inorg. Chem.* **54** 6928; (c) Orthaber A, Karnahl M, Tschierlei S, Streich D, Stein M and Ott S 2014 Coordination and conformational isomers in mononuclear iron complexes with pertinence to the [FeFe] hydrogenase active site *Dalton Trans.* **43** 4537; (d) Dey S, Das P K and Dey A 2013 Mononuclear iron hydrogenase *Coord. Chem. Rev.* **257** 42
5. (a) Ghosh S, Basak-Modi S, Richmond M G, Nordlander E and Hogarth G 2018 Electrocatalytic proton reduction by thiolate-capped triiron clusters $[Fe_3(CO)_9(\mu_3\text{-SR})(\mu\text{-H})]$ (R=$^{i}$Pr, $^{t}$Bu) *Inorg. Chim. Acta* **480** 47; (b) Lunsford A M, Beto C C, Ding S, Erdem Ö F, Wang N, Bhuvanesh N, Hall M B and Darensbourg M Y 2016 Cyanide-bridged iron complexes as biomimetics of triiron arrangements in maturases of the H cluster of the di-iron hydrogenase *Chem. Sci.* **7** 3710; (c) Beaume L, Clémancey M, Blondin G, Greco C, Pétillon F Y, Schollhammer P and Talarmin J 2014 New Systematic Route to Mixed-Valence Triiron Clusters Derived from Dinuclear Models of the Active Site of [Fe−Fe]-Hydrogenases *Organometallics* **33** 6290; (d) Rahaman A, Ghosh S, Unwin D G, Basak-Modi S, Holt K B, Kabir S E, Nordlander E, Richmond M G and Hogarth G 2014 Bioinspired Hydrogenase Models: The Mixed-Valence Triiron Complex $[Fe_3(CO)_7(\mu\text{-edt})_2]$ and Phosphine Derivatives $[Fe_3(CO)_{7-x}(PPh_3)_x(\mu\text{-edt})_2]$ (x=1, 2) and $[Fe_3(CO)_5(\kappa^2\text{-diphosphine})(\mu\text{-edt})_2]$ as Proton Reduction Catalysts *Organometallics* **33** 1356
6. (a) Abul-Futouh H, Almazahreh L R, Harb M K, Görls H, El-khateeb M and Weigand W 2017 [FeFe]-Hydrogenase H-Cluster Mimics with Various -$S(CH_2)_nS$- Linker Lengths (n=2−8): A Systematic Study *Inorg. Chem.* **56** 10437; (b) Abul-Futouh H, Görls H and Weigand W 2017 A new macrocyclic [FeFe]-hydrogenase H cluster model *Phosphorus Sulfur Silicon Relat. Elem.* **192** 634; (c) Abul-Futouh H, Almazahreh L R, Sakamoto T, Stessman N Y T, Lichtenberger D L, Glass R S, Görls H, Elkhateeb M, Schollhammer P, Mloston G and Weigand W 2017 [FeFe]-Hydrogenase H-Cluster Mimics with Unique Planar $\mu\text{-}(SCH_2)_2ER_2$ Linkers (E=Ge and Sn) *Chem. Eur. J.* **23** 346
7. Liu Y C, Tu L K, Yen T H, Lee G H and Chiang M H 2011 Influences on the rotated structure of diiron dithiolate complexes: electronic asymmetry vs. secondary coordination sphere interaction *Dalton Trans.* **40** 2528
8. Apfel U P, Halpin Y, Görls H, Vos J G, Schweizer B, Linti G and Weigand W 2007 Synthesis and Characterization of Hydroxy-Functionalized Models for the Active Site in Fe-Only-Hydrogenases *Chem. Biodivers.* **4** 2138
9. Zhang Y, Si Y T, Hu M Q, Chen C N and Liu Q T 2007 Bis($\mu_4$-butane-1,4-dithiolato)bis[hexacarbonyldi-iron(II)(Fe-Fe)] *Acta Cryst.* **C63** 499
10. Song L C, Gao J, Wang H T, Hua Y J, Fan H T, Zhang X G and Hu Q M 2006 Synthesis and Structural Characterization of Metallocrown Ethers Containing Butterfly $Fe_2S_2$ Cluster Cores. Biomimetic Hydrogen Evolution Catalyzed by $Fe_2(\mu\text{-}SCH_2CH_2OCH_2CH_2S\text{-}\mu)(CO)_6$ *Organometallics* **25** 5724
11. Johnson S L, Gerasimchuk N N and Mebi C A 2018 Cyclic tetranuclear iron-carbonyl complex containing thiobisbenzenethiolate ligands: Synthesis and structural characterization *Inorg. Chim. Acta* **477** 306
12. Song L C, Qi C H, Bao H L, Fang X N and Song H B 2012 Synthetic and Structural Investigations on Some New 1,2,4,5-$(CH_2)_4C_6H_2$ Moiety-Containing Butterfly Fe/S Cluster Complexes from Reactions of Tetrathiol 1,2,4,5-$(HSCH_2)_4C_6H_2$ with $Fe_3(CO)_{12}$ or with $Fe_3(CO)_{12}$ in the Presence of $Et_3N$ *Organometallics* **31** 5358
13. Chen L, Wang M, Gloaguen F, Zheng D, Zhang P and Sun L 2012 Multielectron-Transfer Templates via Consecutive Two-Electron Transformations: Iron-Sulfur Complexes Relevant to Biological Enzymes *Chem. Eur. J.* **18** 13968
14. (a) Li Y L, Xie B, Zou L K, Lin X and Zhu S S 2013 Synthesis, Characterization, and X-ray Crystal Structure of Macrocyclic Nickel/Iron/Sulfur Cluster Complexes *Z. Anorg. Allg. Chem.* **639** 1011; (b) Song L C, Li Y L, Li L, Gu Z C and Hu Q M 2010 Synthetic and Structural Investigations of Linear and Macrocyclic Nickel/Iron/Sulfur Cluster Complexes *Inorg. Chem.* **49** 10174; (c) Song L C, Fang X N, Li C G, Yan J, Bao H L and Hu Q M 2008 Novel μ-CO-Containing Butterfly Fe/S Cluster Anions Generated from Tetrathiols, $Fe_3(CO)_{12}$, and $Et_3N$: Their Reactions with Electrophiles To Give Neutral Butterfly Fe/S Cluster Complexes *Organometallics* **27** 3225; (d) Song L C, Fan H T, Hu Q M, Yang Z Y, Sun Y and Gong F H 2003 Formation and Chemical Reactivities of a New Type of Double-Butterfly $[\{Fe_2(\mu\text{-CO})(CO)_6\}_2(\mu\text{-SZS-}\mu)]^{2-}$: Synthetic and Structural Studies on Novel Linear and Macrocyclic Butterfly Fe/E (E=S, Se) Cluster Complexes *Chem. Eur. J.* **9** 170
15. (a) Karnahl M, Orthaber A, Tschierlei S, Nagarajan L and Ott S 2012 Structural and spectroscopic characterization of tetranuclear iron complexes containing a $P_2^RN_2^{Ph}$ bridge *J. Coord. Chem.* **65** 2713; (b) Song L C, Gao W, Luo X, Wang Z X, Sun X J and Song H B 2012 Synthesis, Characterization, and Electrochemical Properties of Benzyloxy-Functionalized Diiron 1,3-Propanedithiolate Complexes Relevant to the Active Site of [FeFe]-Hydrogenases *Organometallics* **31** 3324; (c) Wen N, Xu F, Feng Y and Du S 2011 A new cumulene diiron complex related to the active site of Fe-only hydrogenases and its phosphine substituted derivatives: Synthesis, electrochemistry and structural characterization *J. Inorg. Biochem.* **105** 1123; (d) Liu X F

and Yin B S 2010 Synthesis and structural characterization of a diiron propanedithiolate complex [(μ-PDT)$Fe_2(CO)_5$]$_2$[($\eta^5$-$Ph_2PC_5H_4$)$_2$Fe] containing a bidentate phosphine ligand 1,1'-bis(diphenylphosphino)ferrocene *J. Coord. Chem.* **63** 4061
16. Liu Y C, Tu L K, Yen T H, Lee G H, Yang S T and Chiang M H 2010 Secondary Coordination Sphere Interactions within the Biomimetic Iron Azadithiolate Complexes Related to Fe-Only Hydrogenase: Dynamic Measure of Electron Density about the Fe Sites *Inorg. Chem.* **49** 6409
17. Chen L, Wang M, Gloaguen F, Zheng D, Zhang P and Sun L 2013 Tetranuclear Iron Complexes Bearing Benzenetetrathiolate Bridges as Four-Electron Transformation Templates and Their Electrocatalytic Properties for Proton Reduction *Inorg. Chem.* **52** 1798
18. Gao W, Liu J, Ma C, Weng L, Jin K, Chen C, Åkermark B and Sun L 2006 Synthesis, structures and electrochemical properties of amino-derivatives of diiron azadithiolates as active site models of Fe-only hydrogenase *Inorg. Chim. Acta* **359** 1071
19. Gao W, Liu J, Åkermark B and Sun L 2006 Bidentate Phosphine Ligand Based $Fe_2S_2$-Containing Macromolecules: Synthesis, Characterization, and Catalytic Electrochemical Hydrogen Production *Inorg. Chem.* **45** 9169
20. Gao W, Ekström J, Liu J, Chen C, Eriksson L, Weng L, Åkermark B and Sun L 2007 Binuclear Iron-Sulfur Complexes with Bidentate Phosphine Ligands as Active Site Models of Fe-Hydrogenase and Their Catalytic Proton Reduction *Inorg. Chem.* **46** 1981
21. Natarajan M, Kaim V, Kumar N and Kaur-Ghumaan S 2018 A tetranuclear iron complex: substitution with triphenylphosphine ligand and investigation into electrocatalytic proton reduction *J. Chem. Sci.* **130** 126
22. Chiang M H, Liu Y C, Yang S T and Lee G H 2009 Biomimetic Model Featuring the NH Proton and Bridging Hydride Related to a Proposed Intermediate in Enzymatic $H_2$ Production by Fe-Only Hydrogenase *Inorg. Chem.* **48** 7604
23. Teo B K, Wudl F, Hauser J J and Kruger A 1977 Reactions of tetrathionaphthalene with transition metal carbonyls. Synthesis and characterization of two new organometallic semiconductors $(C_{10}H_4S_4Ni)_x$ and $[C_{10}H_4S_4Co_2(CO)_2]_x$ and a tetrairon cluster $C_{10}H_4S_4Fe_4(CO)_{12}$ *J. Am. Chem. Soc.* **99** 4862
24. Song L C, Fan H T and Hu Q M 2002 The First Example of Macrocycles Containing Butterfly Transition Metal Cluster Cores via Novel Tandem Reactions *J. Am. Chem. Soc.* **124** 4566
25. Chong D, Georgakaki I P, Mejia-Rodriguez R, Sanabria-Chinchilla J, Soriaga M P and Darensbourg M Y 2003 Electrocatalysis of hydrogen production by active site analogues of the iron hydrogenase enzyme: structure/function relationships *Dalton Trans.* 4158
26. Petro B J, Vannucci A K, Lockett L T, Mebi C, Kottani R, Gruhn N E, Nichol G S, Goodyer P A J, Evans D H, Glass R S and Lichtenberger D L 2008 Photoelectron spectroscopy of dithiolatodiironhexacarbonyl models for the active site of [Fe–Fe] hydrogenases: Insight into the reorganization energy of the "rotated" structure in the enzyme *J. Mol. Struct*. **890** 281
27. Elgrishi N, Rountree K J, McCarthy B D, Rountree E S, Eisenhart T T and Dempsey J L 2018 A Practical Beginner's Guide to Cyclic Voltammetry *J. Chem. Educ.* **95** 197
28. Rountree E S, McCarthy B D, Eisenhart T T and Dempsey J L 2014 Evaluation of Homogeneous Electrocatalysts by Cyclic Voltammetry *Inorg. Chem.* **53** 9983
29. Connor G P, Mayer K J, Tribble C S and McNamara W R 2014 Hydrogen Evolution Catalyzed by an Iron Polypyridyl Complex in Aqueous Solutions *Inorg. Chem.* **53** 5408
30. Carroll M E, Barton B E, Rauchfuss T B and Carroll P J 2012 Synthetic Models for the Active Site of the [FeFe]-Hydrogenase: Catalytic Proton Reduction and the Structure of the Doubly Protonated Intermediate *J. Am. Chem. Soc.* **134** 18843
31. (a) Roy S, Mazinani S K S, Groy T L, Gan L, Tarakeshwar P, Mujica V and Jones A K 2014 Catalytic Hydrogen Evolution by Fe(II) Carbonyls Featuring a Dithiolate and a Chelating Phosphine *Inorg. Chem.* **53** 8919; (b) McNamara W R, Han Z, Alperin P J, Brennessel W W, Holland P L and Eisenberg R 2011 A Cobalt-Dithiolene Complex for the Photocatalytic and Electrocatalytic Reduction of Protons *J. Am. Chem. Soc.* **133** 15368
32. (a) Costentin C, Dridi H and Savéant J M 2014 Molecular Catalysis of $H_2$ Evolution: Diagnosing Heterolytic versus Homolytic Pathways *J. Am. Chem. Soc*. **136** 13727; (b) Costentin C, Robert M and Savéant J M 2013 Catalysis of the electrochemical reduction of carbon dioxide *Chem. Soc. Rev*. **42** 2423
33. McCarthy B D, Martin D J, Rountree E S, Ullman A C and Dempsey J L 2014 Electrochemical Reduction of Brønsted Acids by Glassy Carbon in Acetonitrile-Implications for Electrocatalytic Hydrogen Evolution *Inorg. Chem.* **53** 8350
34. Fourmond V, Jacques P A, Fontecave M and Artero V 2010 $H_2$ Evolution and Molecular Electrocatalysts: Determination of Overpotentials and Effect of Homoconjugation *Inorg. Chem.* **49** 10338
35. Fu L Z, Zhou L L, Tang L Z, Zhang Y X and Zhan S Z 2015 A molecular iron(III) electrocatalyst supported by amine-bis(phenolate) ligand for water reduction *Int. J. Hydrogen Energy* **40** 8688
36. Costentin C, Drouet S, Robert M and Savéant J M 2012 Turnover Numbers, Turnover Frequencies, and Overpotential in Molecular Catalysis of Electrochemical Reactions. Cyclic Voltammetry and Preparative-Scale Electrolysis *J. Am. Chem. Soc.* **134** 11235
37. Artero V and Savéant J M 2014 Toward the rational benchmarking of homogeneous $H_2$-evolving catalysts *Energy Environ. Sci*. **7** 3808
38. Hu C and Fan W Y 2019 Molybdenum carbonyl complexes as HER electrocatalysts *Mol. Catal.* **479** 110615
39. Agarwal T and Kaur-Ghumaan S 2020 Mono- and dinuclear mimics of the [FeFe] hydrogenase enzyme featuring bis(monothiolato) and 1,3,5-triaza-7-phosphaadamantane ligand *Inorg. Chim. Acta* **504** 119442